AEM
Journals.ASM.org

Characterization of *Pleurotus ostreatus* Biofilms by Using the Calgary Biofilm Device

Lorena Pesciaroli,[a] Maurizio Petruccioli,[a] Stefano Fedi,[b] Andrea Firrincieli,[b] Federico Federici,[a] Alessandro D'Annibale[a]

Department for Innovation in Biological, Agro-Food, and Forestry Systems, University of Tuscia, Viterbo, Italy[a]; Department of Pharmacy and Biotechnology, University of Bologna, Bologna, Italy[b]

The adequacy of the Calgary biofilm device, often referred to as the MBEC system, as a high-throughput approach to the production and subsequent characterization of *Pleurotus ostreatus* biofilms was assessed. The hydroxyapatite-coating of pegs was necessary to enable biofilm attachment, and the standardization of vegetative inocula ensured a uniform distribution of *P. ostreatus* biofilms, which is necessary for high-throughput evaluations of several antimicrobials and exposure conditions. Scanning electron microscopy showed surface-associated growth, the occurrence of a complex aggregated growth organized in multilayers or hyphal bundles, and the encasement of hyphae within an extracellular matrix (ECM), the extent of which increased with time. Chemical analyses showed that biofilms differed from free-floating cultures for their higher contents of total sugars (TS) and ECM, with the latter being mainly composed of TS and, to a lesser extent, protein. Confocal laser scanning microscopy analysis of 4-day-old biofilms showed the presence of interspersed interstitial voids and water channels in the mycelial network, the density and compactness of which increased after a 7-day incubation, with the novel occurrence of ECM aggregates with an α-glucan moiety. In 4- and 7-day-old biofilms, tolerance to cadmium was increased by factors of 3.2 and 11.1, respectively, compared to coeval free-floating counterparts.

In nature, microorganisms exhibit a frequent tendency to interact with solid matrices and other microbes so as to develop complex systems usually referred to as biofilms. Thus, biofilm formation is one of the most widespread growth strategies of microbiota in natural ecosystems (1).

Since fungal biofilms do not accurately meet the stringent biofilm definitions based on bacterial models, a set of structural and phenotypic criteria for these systems has been recently proposed by Harding et al. (2). In particular, the former set comprises surface-associated growth, the encasement of hyphae within a self-produced extracellular matrix (ECM) and, finally, the occurrence of a complex aggregated growth involving the presence of either multilayers or hyphal bundles (2). Some studies seem to disengage from the stringent criteria of firm attachment on a surface and suggest that multicellular communities adhering either to each other (3) or onto the air-liquid interface (4) might also be regarded as fungal biofilms. Thus, a clear differentiation between hyphal aggregates and a proper biofilm state for fungi still appears to be a matter of contentious debate.

The white-rot basidiomycete *Pleurotus ostreatus*, a highly relevant species from both commercial and ecological viewpoints, is known to produce monospecific (5) and mixed (6, 7) biofilms. On the one hand, monospecific *P. ostreatus* biofilms have been successfully used in wastewater treatment (5, 8). On the other hand, mixed biofilm systems involving this species were suggested to have important agronomic implications, such as N fixation (9), endophytic colonization (7), and rock phosphate solubilization (6).

An additional issue to be addressed is whether *P. ostreatus* biofilms exhibit increased ability to cope with ubiquitous contaminants, such as heavy metals, a common property of microbial biofilms (10, 11). Due to the widely reported *P. ostreatus* ability to degrade a wide array of xenobiotics (8, 12), this has important repercussions in the mycoremediation of contaminated sites and wastewater treatment where mixed scenarios of contamination involving inorganic and organic pollutants are often observed (13). Among the former group of contaminants, cadmium is one of the most ubiquitous and toxic components of industrial and municipal wastes with potential carcinogenic and mutagenic effects (13–15).

The Calgary biofilm device (CBD), originally used for high-throughput testing of microbe susceptibility to biocides (16), has been reported to enable structure-function biofilm studies under a variety of growth and exposure conditions. Basically, this system consists of a polystyrene lid with 96 downward-protruding pegs that can be adapted to either a standard 96-well microtiter plate or a multichannel trough tray. It has been extensively used for the study of bacterial biofilms (16, 17) and of some fungi, such as *Candida* and *Cryptococcus* species (18, 19) and *Aspergillus fumigatus* (19). Conversely, the use of the CBD in biofilm studies of white-rot basidiomycetes has not yet been reported likely due to two main concomitant reasons. First, and unlike bacteria and yeasts, a reliable and uniform application of their inocula to such low-volume systems is constrained by the objective difficulties of dispensing mycelial suspensions, unless spores are used. Second, the strong tendency of basidiomycetes to readily form free-floating mycelial agglomerates might prevent the formation of an uniform biofilm, namely, a consistent peg to peg cell density (19).

Thus, in the present investigation, the adequacy of the CBD as a high-throughput approach to the production and subsequent characterization of *P. ostreatus* biofilms was assessed. The specific objectives of the present study were (i) to find suited conditions

Received 26 June 2013 **Accepted** 22 July 2013
Published ahead of print 26 July 2013
Address correspondence to Alessandro D'Annibale, dannib@unitus.it.

doi:10.1128/AEM.02099-13

leading to biofilm production and to its even distribution, (ii) to compare chemical and structural biofilm properties with respect to its coeval free-floating counterpart, and (iii) to assess whether the biofilm exhibited a greater ability to endure the toxic effects of cadmium than free-floating cultures. The achievement of the second and third objectives also served the purpose of determining whether free-floating mycelial aggregates (i.e., pellets) possibly met the requirements of a biofilm. To this aim, the Luria-Bertani (LB) medium was chosen as the growth medium due to its established use in studies of metal resistance (20) and in view of future implementation of mixed biofilms involving *P. ostreatus* and bacteria, the relevance of which, from an application point of view, has been shown (6, 7, 9). The endpoints for comparisons were set at 4 and 7 days after the inoculation since, at these times, *P. ostreatus* free-floating cultures, grown on LB medium, were in the mid-exponential phase and at the beginning of the stationary phase, respectively (21). Despite the aforementioned applications of *P. ostreatus* monospecific and mixed biofilm findings, with a sole exception (21), no basic information regarding physiological and structural properties of biofilm systems of this species is available yet.

MATERIALS AND METHODS

Materials and growth media. An MBEC physiology and genetics assay device with either 96 polystyrene (P&G) or 96 hydroxyapatite-coated (HA-P&G) pegs combined with conventional 96-well plates was purchased from Innovotech, Inc. (Edmonton, Canada). 3-[4,5-Dimethylthiazol-2-yl]-2,5-diphenyltetrazolium bromide (MTT) was obtained from Sigma (Milan, Italy). ACS reagent-grade cadmium sulfate and reduced glutathione (GSH) were purchased from Sigma-Aldrich (Milan, Italy). All stock solutions, prepared in Milli-Q water, were passed through a 0.22-μm-pore-size syringe filter, transferred into sterile glass vials, and stored at room temperature. In the case of cadmium sulfate, a stock solution was prepared in LB medium at the highest concentration used in the challenge plate (i.e., 30 mM).

Microorganism and inoculum production and standardization. *P. ostreatus* (Jacquin: Fr.) Kummer, strain ATCC 58052, was stored a 4°C and periodically subcultured on malt extract agar (MEA). Mycelium fragments were scraped from 10-day-old MEA slants, suspended in sterile deionized water, and then homogenized using a sterile Potter homogenizer to yield a 10-g liter^{-1} suspension. Erlenmeyer flasks (500 ml) containing 95 ml of malt extract glucose medium (10 g of glucose and 5 g of malt extract liter^{-1}) were inoculated with these cell suspensions (5 ml per flask) and incubated on a rotary shaker (150 rpm, 28°C) for 120 h. The precultures were homogenized with an Ultra-Turrax T18 (IKA Labortechnik, Staufen, Germany), varying the speed (i.e., from 3,000 to 7,000 rpm), homogenization time per cycle (i.e., from 5 to 30 s), and number of homogenization cycles (i.e., from 1 to 2). Regardless of the tested conditions, inocula were maintained on ice during homogenization. Mycelial suspensions were centrifuged (6,000 × *g*, 10 min), washed with deionized water, and centrifuged again as described above, and then suspended again to yield a biomass concentration of ~2.5 g (dry weight) liter^{-1}. Then, 30-μl inocula were applied to a standard 96-well plate using a multichannel pipette, the tips of which had been modified by deleting the 3-mm distal portion. Next, both the viability and the uniformity of distribution of inocula among wells were tested by an MTT reduction assay (see below).

Biofilm formation on an MBEC physiology and genetics assay device. Experiments were conducted with plastic lids endowed with either polystyrene or hydroxyapatite-coated pegs. For both configurations, each well was loaded with 150 μl of LB medium, and 30 μl of inoculum was applied by using a multichannel pipette, the tips of which had been modified as described above. The whole assembly was then incubated at 30°C for 4 or 7 days under orbital shaking (150 rpm).

At the end of each experiment, nonsessile or loosely bound biomass was removed by transferring the plastic lid to a standard 96-well tray, each one containing 180 μl of phosphate-buffered saline (PBS), followed by incubation for 15 min under orbital shaking (70 rpm). The washing procedure with PBS was repeated three times.

Free-floating culture conditions. *P. ostreatus* free-floating cultures were obtained in 96-well polystyrene plates (CellStar; Greiner Bio-One, Germany). In particular, 30 μl of inoculum was applied by using a multichannel pipette, the tips of which had been modified as described above, onto each well containing LB medium (150 μl), followed by incubation at 30°C for either 4 or 7 days under orbital shaking (150 rpm).

MTT reduction assay. Due to the impossibility of gravimetrically determining the amount of biofilm on each peg, an assay involving the reduction of a tetrazolium salt to its corresponding formazan was used (22). In particular, at the end of the biofilm experiments, the plastic lid of the CBD bearing colonized pegs was transferred to another standard 96-well tray, each well of which containing 180 μl of MTT solution (5 mg ml of PBS^{-1}), previously equilibrated at 37°C. The plate was incubated at the same temperature for 5 h in the dark, and the formazan produced was solubilized for 15 min with a dimethyl sulfoxide–0.2 M glycine buffer (pH 8.6) mixture (6:1 [vol/vol]) in an Ultrasonic 220 bath (Bransonic, USA). The pooled extracts were read at 578 nm (ε = 16,900 M^{-1} cm^{-1}). This assay was also used as a residual metabolic index for cadmium susceptibility testing (see below). In the case of free-floating cultures, the growth medium, PBS, and spent MTT solution were separated from biomass by centrifugation (3,500 × *g*, 3 min, 4°C) in a refrigerated Sorvall Legend X1R apparatus (Thermo Fisher Scientific, Osterode, Germany) equipped with a M-20 microplate swinging bucket rotor, followed by removal of the supernatant using a multichannel pipette.

Chemical analyses of biofilms and free-floating cultures. Wet biomass of biofilm and free-floating cultures (~10 mg [dry weight]) were suspended in 5 ml of double-distilled water and homogenized with Ultra-Turrax T8 (IKA-Werk, Staufen, Germany) for 2 min at 8,000 rpm. The suspensions thus obtained were analyzed for their total sugar, glucosamine, total protein, and lipid content. One milliliter of 18.4 M H_2SO_4 was added dropwise to the homogenate (1 ml), and the mixture was incubated at room temperature for 15 min prior to the determination of total sugars by the anthrone-sulfuric acid method (23). Glucosamine was determined by the method of Chen and Johnson (24); in particular, 1 ml of homogenate was added along with 1 ml of HCl (12 N), and the suspension incubated at 100°C for 4 h in screw-cap Teflon-lined tubes. Hydrolysates were then reacted with the Ehrlich reagent (1.6 g of *N*,*N*-dimethyl-*p*-aminobenzaldehyde in 60 ml of a 1:1 [vol/vol] ethanol–12 N HCl mixture), and a calibration curve was built with glucosamine hydrochloride (range, 0 to 40 μg). Lipids were determined in the homogenates (0.25 to 1.0 ml) by the vanillin-phosphoric reagent according to the method of Izard and Limberger (25) using triolein as the standard (0 to 100 μg). Protein was determined by a modification of the method of Phillips and Gordon (26). In particular, samples (2 mg [dry weight]) were first incubated for 8 h at 40°C in 1.0 N NaOH containing 0.1% (wt/vol) Triton X-100 under magnetic stirring, and the incubation mixture was subsequently neutralized with 6 N HCl prior to centrifugation (8,000 × *g*, 5 min). The supernatant was then analyzed by the dye-binding method (27), and bovine serum albumin used as the standard (range, 0 to 25 μg). The ash content was determined after ignition of samples in a muffle furnace at 550°C for 8 h. The ECM in biofilm and free-floating biomass was extracted and quantified by the method of Liu and Fang (28). In particular, samples (1.5 to 2.0 g [wet weight]) were incubated under static conditions in 10 ml of double-distilled water containing 60 μl of formaldehyde (37%) for 1 h at 4°C. After the addition of 4 ml of 1.0 N NaOH, the mixture was further incubated for 3 h at 4°C. After centrifugation (11,000 × *g*, 20 min) at 4°C, the supernatant was passed through a 0.2-μm-pore-size filter (Sartorius Stedim Biotech, Goettingen, Germany), and the filtrate was dialyzed against double-

distilled water for 12 h at 4°C. The total quantity of extracted ECM was gravimetrically determined after lyophilization, and the samples were then analyzed for their total sugar, protein, glucosamine, and lipid content as described above.

Cadmium susceptibility testing. Fungal biofilm and free-floating cell susceptibility to cadmium was expressed here by the MIC (MIC_{90}) and minimum fungicidal concentration (MFC) defined as the lowest concentrations leading to 90 and 99% inhibitions of metabolic activity, respectively. The former and latter parameters were determined immediately after the exposure and after a recovery phase in the challenging medium in the absence of the toxicant, respectively. Metal susceptibility assays were performed using the CBD assay according to a modification of the procedure described by Harrison et al. (29). In each assay, 10 concentrations of cadmium (i.e., 0, 0.5, 1.0, 2.0, 5.0, 10, 15, 20, 25, and 30 mM) were tested against the biofilms grown on the 96 pegs of the CBD. The peripheral columns containing uninoculated LB medium were used as microbial contamination controls. Each Cd concentration was tested in eight replicates. After 4 or 7 days of growth, both biofilms and free-floating cultures were rinsed twice in PBS and then exposed to Cd in the same medium used for growth. In the case of the latter cultures, each rinsing step was followed by centrifugation, as described in the MTT reduction subsection. The exposure was carried out at 30°C in an orbital shaker (150 rpm) for 48 h. For the MIC_{90} determination, after exposure, biofilms and coeval free-floating cultures were rinsed twice with PBS for 15 min under agitation and immediately subjected to the MTT reduction assay. In order to determine the MFC, both culture systems were transferred into a neutralization plate containing PBS added with 5.0 mM GSH and then incubated for 30 min. At the end of the neutralization phase, cultures were transferred to the recovery plate containing fresh LB medium and subsequently incubated for 5 days, as described above. At the end of the incubation, both biofilm and free-floating cultures were washed with sterile PBS as described above and subsequently analyzed for residual viability. In particular, the MTT reduction data (f) were plotted against respective exposure metal concentrations [Cd, mM] and data fitted by a two-term exponential decay function: $f = a \cdot e^{-k[\mathrm{Cd}]}$, where a is the amount of reduced formazan in unexposed cultures, and k is the exponential decay coefficient. The goodness of fit of each of the curves thus obtained was checked by the values of coefficient of determination adjusted by the degrees of freedom, the significance levels (P) of the a and k parameters, the standard error of the estimate of the model, and the Fisher-Snedecor coefficient of the regression.

Scanning electron microscopy (SEM). Three replicate pegs of *P. ostreatus* biofilm, grown for either 4 or 7 days, were detached from the lid with the aid of a plier and immediately prefixed for 30 min at 4°C in 0.1 M cacodylate buffer (pH 7.3) containing 2.5% glutaraldehyde (buffer A) and added with 0.075% ruthenium red (wt/vol) and 0.075 M lysine acetate (30). After washing with buffer A (3 changes for 10 min, each at 4°C), specimens were fixed with buffer A for 2 h at 4°C. The washing step with buffer A was repeated as described above, and specimens were then post-fixed with 2% osmium tetroxide in buffer A for 2 h at 4°C, washed in the same buffer (3 changes for 15 min each at 4°C), and then dehydrated in a graded ethanol series (31). Samples were dried by the critical point method using CO_2 in a Balzers Union CPD 020 (Vaduz, Liechtenstein). The samples were attached to aluminum stubs using a carbon tape and sputter coated with gold in a Balzers MED 010 unit. The observation was made by a JSM 6010 LA analytical SEM featuring integrated energy dispersive spectroscopy (EDS; JEOL, Tokyo, Japan).

Transmission electron microscopy (TEM). Samples were fixed and dehydrated as described above and then infiltrated for 3 days with decreasing ethanol-LR White resin (SPI Supplies, West Chester, PA) ratios. At the end of the procedure, samples were embedded in LR White resin and cut with a Reichert Ultracut ultramicrotome (Leica Microsystems Srl, Milan, Italy) using a diamond knife. Thin sections (60 to 80 nm) were collected on copper grids, stained with uranyl acetate and lead citrate, and observed with a JEOL 1200 EX II electron microscope (JEOL). Micrographs were acquired by the Olympus SIS VELETA charge-coupled device camera equipped with iTEM software (Olympus Soft Imaging Solutions GmbH, Muenster, Germany).

Confocal laser scanning microscopy (CLSM). Triplicate pegs on which *P. ostreatus* biofilms had developed for either 4 or 7 days of incubation were washed in PBS for 1 min and fixed with PBS containing 5% glutaraldehyde (wt/vol) for 50 min; the pegs were then washed twice with 0.9% NaCl solution. Each peg was incubated for 15 min at 37°C in 4 ml of 0.9% NaCl containing 0.02% concanavalin A conjugated to Texas Red (CATR; Molecular Probes, Inc., Eugene, OR). Each peg was washed in 0.9% NaCl solution for few seconds and dipped for 10 s in 0.002% (wt/vol) Calcofluor White Stain M2R (CFW; Fluka) in 0.9% NaCl. CATR binds to α-mannopyranosyl and α-glucopyranosyl residues with red fluorescence, whereas CFW binds to β-glucans and chitin. After incubation with the dyes, pegs were observed with a TCS SL Leica confocal scanning laser microscope equipped with argon and HeNe lasers. The objective was a PL-Apochromat lens (40×; numerical aperture, 0.75). Depth measurements were taken at regular intervals across the width of the device. To determine the structure of 4- and 7-day-old biofilms, a series of 30 (x-y) optical sections with a thickness of 1.3 μm were taken along the z axis. Confocal images of green (CFW) and red (CATR) fluorescence were conceived simultaneously using a multi-track mode. A geometric representation of the biofilm surfaces, termed the "isosurface," was computed using the Amira 5.4.5 software package (Visualization Sciences Group, Burlington, NE) (32). For the x-y, x-z, and y-z views, images were processed using volume rendering computation analysis (32).

P. ostreatus biofilms were also stained with FUN-1 viability probe (Molecular Probes, Inc.). Each peg was rinsed as described above and stained in 10 mM HEPES buffer (pH 7.2) containing 25 μM FUN-1 and 2% D-glucose. In metabolically active cells, the FUN-1 probe is converted to orange-red cylindrical intravacuolar structures (CIVS), which emit a bright red fluorescent light (emission ≥ 530 nm) if excited at 480 nm. CIVS formation only occurs in metabolically active cells, whereas dead cells show a bright and diffuse green-yellow fluorescence.

Statistical analysis. The uniformity of distribution of adherent biomass onto pegs was assessed by one-way analysis of variance, followed by *post hoc* multiple pairwise comparisons of column means by the HSD-Tukey test ($P \leq 0.05$).

RESULTS

Biofilm production on MBEC devices. Inoculum standardization experiments established that the use of two homogenization cycles, each one lasting 15 s at a speed of 7,000 rpm, yielded highly vital mycelial suspensions and enabled their use at the level of few microliter volumes (25 to 45 μl) without impairing the reproducibility of application along wells. This was assessed by determining the MTT reduction on each well immediately downstream of the inoculum application and comparing data by multiple pairwise comparison using a *post hoc* Tukey test; in this respect, both column and row means did not significantly differ at a confidence level of 95% (data not shown). An increase in either homogenization speed or cycle duration with respect to the above-mentioned conditions had a severe detrimental effect on viability.

The CBD with polystyrene pegs was not suitable for the formation of a stable biofilm, and mycelial biomass was readily removed at the end of incubation by washes with PBS in either a free-floating or a loosely bound form. Thus, modified plates endowed with hydroxyapatite (HA)-coated pegs were used in subsequent experiments. With this adjustment, an even distribution of biofilms was obtained, as inferred from the lack of statistically significant differences among column means of MTT reduction at both 4 and 7 days postinoculation (Fig. 1). The increase over time of sessile biomass, as determined from visual inspections, was asso-

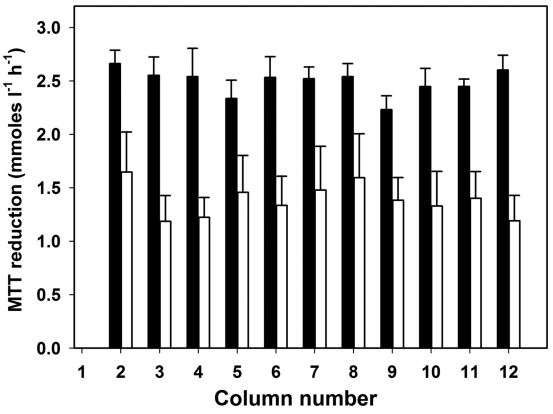

FIG 1 Average *P. ostreatus* biofilm production, inferred by MTT reduction, on column pegs of the MBEC P&G device after 4 (■) and 7 days (□) growth on the LB medium at 30°C under orbital shaking (150 rpm). The data represent means ± the standard deviations of quadruplicate plates.

ciated with higher MTT-reducing ability in 7- than in 4-day-old biofilms (Fig. 1).

Comparative chemical characterization of biofilm and free-floating *P. ostreatus* biomass. In free-floating and biofilm cultures, protein and total lipid contents decreased and increased, respectively, as the incubation time was extended from 4 to 7 days; however, no significant differences in these parameters were observed by comparing coeval culture systems (Fig. 2). Although the same time-dependent increase was observed for chitin content, the biofilms generally exhibited lower contents than coeval free-floating cultures. The most substantial differences between biofilms and coeval free-floating cultures were observed in their respective total sugars and ECM contents (Fig. 2). Although in both culture systems the former parameter markedly increased as a function of the incubation time, the biofilms displayed a higher total sugar content than their coeval free-floating counterparts. Regardless of culture age, free-floating cultures showed low and steady ECM contents (i.e., 3.1 and 3.6% in 4- and 7-day-old cultures, respectively). In biofilms, instead, the amount of extractable ECM increased over time passing from 6.1 to 11.2% after 4 and 7 days incubation. Regardless of both the time and the culture system, ECM was made up of total sugars and, to a lesser extent, of protein, whereas other components were undetectable. In particular, the highest and lowest total sugar and protein contents, respectively, were found in 7-day-old biofilms.

Morphostructural analysis of *P. ostreatus* biofilms. Biofilms were examined *in situ* using both scanning/transmission electron microscopy and CLSM. SEM pictures show that after 4 days of incubation, *P. ostreatus* developed a very thin layer of adherent biomass (Fig. 3A) made of a highly intertwined mycelial network with interspersed empty channels (Fig. 3B and Fig. 4A and B). The biofilm's constituent hyphae had an average diameter of 1.3 ± 0.1 μm and exhibited a smooth surface with sparse distribution of filaments of ECM (Fig. 3B). Conversely, the thickness in 7-day-old biofilms dramatically increased, exceeding 300 μm in some areas of the biofilm edge at the proximal side of the peg (Fig. 3C); its constituent hyphae exhibited a rough surface and were uniformly lined with an ECM sheath and, as a consequence, their average diameters increased to 3.4 ± 0.2 μm (Fig. 3D). Moreover, the frequent presence of hyphal bundles embedded within the ECM was also observed in 7-day-old biofilms (Fig. 3D, inset, and Fig. 4E and F). However, the peg's surface affected by the biofilm increased only slightly with respect to the earlier harvest. Thus, the observed growth during the incubation time was due to a preferential increase in thickness rather than to a colonization across the

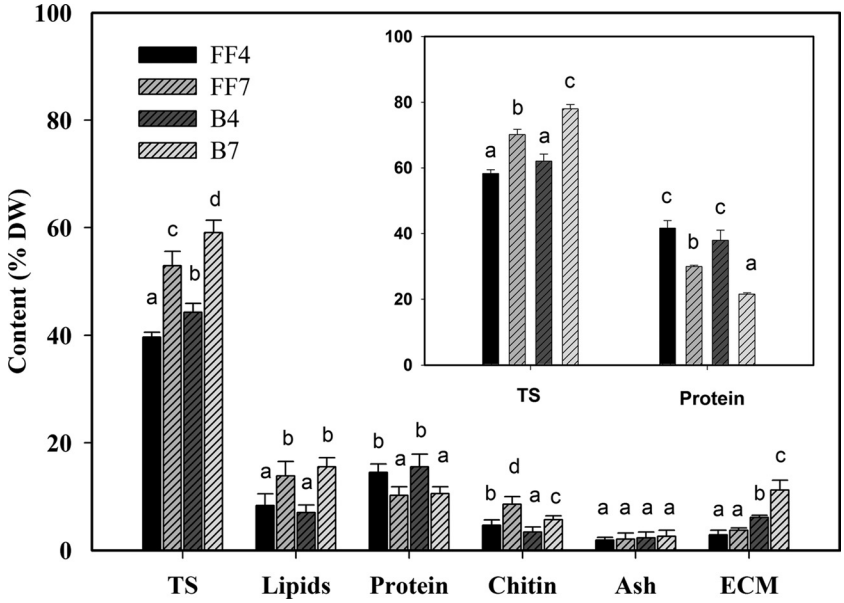

FIG 2 Total sugars (TS), lipid, protein, chitin, and ash contents and percent amounts of extracted ECM in free-floating (FF) and biofilm (B) biomasses after 4 and 7 days incubation in the MBEC P&G system at 30°C under orbital shaking (150 rpm). The inset shows the percent composition, referred to as the ECM dry weight, of protein and TS for each biomass type. With the sole exceptions of ECM and ash, data are the means ± the standard deviations of nine determinations (three replicates for three samples), and same lowercase letters above bars indicate the lack of statistically significant differences for each parameter among culture systems. ECM and ash determinations were performed in triplicate.

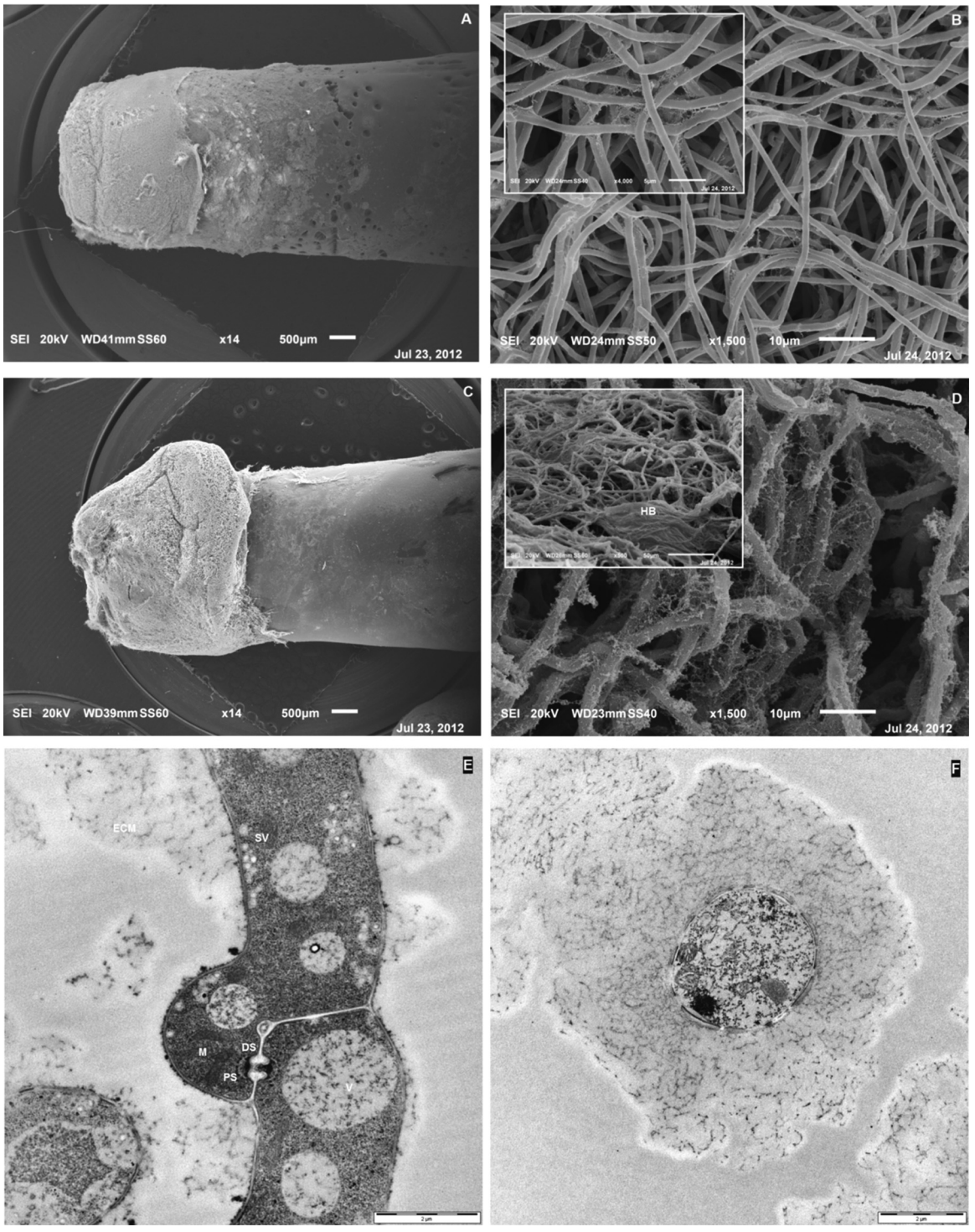

FIG 3 (A to D) SEM micrographs of *P. ostreatus* biofilms grown on the HA-P&G system and LB medium for 4 days (A and B) and 7 days (C and D) at 30°C (150 rpm). Insets show details at higher magnifications. (E and F) TEM micrographs of longitudinal and cross-view sections of a biofilm's constituent hypha, respectively. Abbreviations: DS, dolipore septum; ECM, extracellular matrix; HB, hyphal bundle; PS, parenthosome; SV, secretory vesicles; V, vacuoles.

peg's length. Each peg of the CBD has an approximate surface area of 109 mm^2; its rounded "tip" extends approximately 3 to 5 mm into the growth medium, and thus the "air-liquid-surface interface" occurs approximately 4 to 5 mm above the tip after the inoculated device is agitated on an orbital shaker (32). This means that *P. ostreatus* biofilm was unable to reach and force such an interface.

The TEM image of a 7-day-old constituent hypha shows the presence of both the typical clamp connection and the dolipore septum endowed with parenthosomes that are typical structures

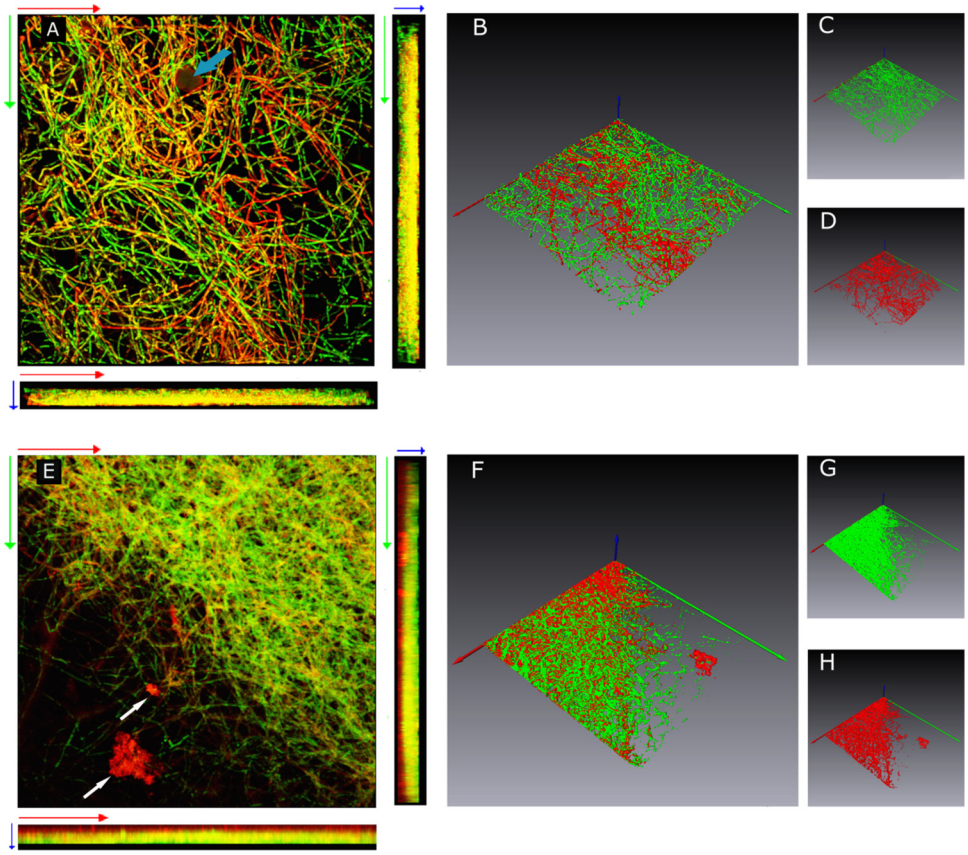

FIG 4 CLSM images of 4-day-old (A to D) and 7-day-old (E to H) *P. ostreatus* biofilms grown on the HA-P&G device under orbital shaking (150 rpm) at 30°C and sequentially stained with concanavalin A conjugated with Texas Red (red emission) and Calcofluor White Stain M2R (green emission). Images A and E are horizontal (*xy*) and vertical side (*xz* and *yz*) views of three-dimensional reconstructed images of 4- and 7-day-old biofilms obtained by volume rendering, respectively, as described by Harrison et al. (32). Isosurfaces of 4- and 7-day-old biofilms are shown in panels B to D and F to H, respectively. Each image represents an area of 375 by 375 μm. The light blue and white arrows in panels A and E indicate a hydroxyapatite granule and ECM aggregates, respectively. The *x*, *y*, and *z* axes are coded in red, green, and blue, respectively. The direction of the blue arrow (*z* axis) is oriented toward the outermost biofilm layers.

of basidiomycetes (Fig. 3E). In addition, significant polysaccharide bundles surrounding the cell wall of the hypha and the accumulation of small secretory vesicles close to the plasma membrane were evident (Fig. 3E). The presence of an ECM sheath uniformly lining an hypha of a 7-day-old biofilm is shown in a cross-view section (Fig. 3F).

The morphostructural organization of *P. ostreatus* biofilms was also investigated by means of CLSM after combined staining with Calcofluor White (CFW) and Texas Red-concanavalin A conjugate (CATR) (33). In 4-day-old biofilms, the architecture of the mycelial network was characterized by the presence of interstitial voids and water channels (Fig. 4A and B). In the same samples, albeit highly intertwined, individual hyphae were fully discernible and found to be responsive to both fluorochromes. In 7-day-old biofilms, an increase in the density of the mycelial network was evident (Fig. 4E and F), and the novel occurrence of CATR-bound ECM aggregates was observed (Fig. 4E). Such an increase in compactness gave rise to the presence of homogeneous, albeit unevenly distributed, red fluorescent ECM zones lining hyphae (Fig. 4F). Interestingly, vertical (*xz* and *yz*) sectioning (side view) of three-dimensional reconstructed images in 7-day-old biofilms showed the preferential accumulation of α-glucan moieties in the innermost biofilm sections while either chitin or β-glucans appeared to predominate in the outermost ones (Fig. 4E). The increase in biofilm compactness, observed in 7-day-old biofilms, did not negatively affect the vitality of hyphae. In fact, from the surface to a depth of ~40 μm, CLSM analyses with the FUN-1 fluorescent probe showed that the frequency of cylindrical intravacuolar structures (CIVS) in 7-day-old biofilms, referred to as a unit of biofilm volume, did not differ from that found in 4-day-old biofilms (data not shown).

Cadmium susceptibility of *P. ostreatus*. Regardless of both culture type and age, the dose-response relationships between Cd concentration and MTT reduction were robustly fitted by a two-term exponential decay function, thus enabling a precise determination of the MIC_{90} and MFC. Table 1 comparatively reports these parameters in coeval biofilm and free-floating cultures, along with the curve-fitting parameters. A higher susceptibility to Cd was evident in 7-day-old versus 4-day-old free-floating cultures; for the former, in fact, the MIC_{90} and MFC values were 3.5- and 2-fold lower than in the latter, respectively. In 4- and 7-day-old biofilms, tolerance to Cd, inferred from the respective MIC_{90}s, was increased by factors of 3.2 and 11.1, respectively, compared to coeval free-floating counterparts. In contrast, we observed 2.4- and 6.5-fold increases in MFC values in 4- and 7-day-old biofilms relative to coeval free-floating cultures (Table 1).

TABLE 1 MICs and MFCs of cadmium in 4- and 7-day-old *P. ostreatus* free-floating and biofilm cultures and related curve-fitting parameters of a two-term exponential decay model[a]

System	MIC parameters				MFC parameters			
	Curve fitting				Curve fitting			
	R^2_{adj}	*F*	*k*	MIC_{90} (mM)	R^2_{adj}	*F*	*k*	MFC (mM)
Free-floating culture								
Four day old	0.933	762.0	0.599 ± 0.027	3.9	0.884[b]	133.97	0.862 ± 0.148	7.0
Seven day old	0.878	231.7	2.114 ± 0.26	1.1	0.848	196.5	0.667 ± 0.084	3.5
Biofilm culture								
Four day old	0.938	1,300.3	0.185 ± 0.008	12.4	0.954	1,561.6	0.137 ± 0.007	16.7
Seven day old	0.979	1,792.7	0.190 ± 0.009	12.2	0.978	2,060.7	0.101 ± 0.004	22.7

[a] R^2_{adj}, coefficient of determination adjusted by the degrees of freedom; *F*, Fisher-Snedecor coefficient; *k*, exponential decay coefficient ± the relative standard error.
[b] Best fit with a three-term exponential decay function.

To assess the possible occurrence of metal-induced structural modifications, free-floating and biofilm cultures were analyzed by SEM after a 48-h exposure to Cd at their respective IC_{90} values. Regardless of their age, the exposure of free-floating cultures to the metal resulted in the novel formation of ECM with a granular appearance, the presence of which, conversely, was not evident on the smooth surfaces of hyphae in coeval unexposed cultures (Fig. 5A versus B and Fig. 5C versus D [4- and 7-day-old cultures, respectively]). Such granular depositions onto the outer surfaces of hyphae did not appear to be due to the possible presence of either Cd crystals or chelates since the presence of the metal was not detected by the integrated EDS analyzer. Another relevant structural change was the occurrence of collapsed hyphae, mainly evident in 4-day-old cultures and likely due to turgor losses. In biofilms, the only modification in Cd-exposed cultures with respect to unexposed counterparts was the appearance of ECM, which changed from an either filamentous or reticular semblance to a granular one. In both exposed free-floating and biofilm cultures, neither an increase in the branching frequency nor in the occurrence of melanized hyphae was observed.

DISCUSSION

The use of high-throughput approaches to microbial biofilms, such as those relying on the CBD, has not yet been used with white-rot basidiomycetes. This is presumably due to two main technical difficulties associated with their filamentous growth mode that might negatively impact on inoculum standardization and uniformity of biofilm formation among pegs. This apparently heavy constraint was overcome in the present study by a proper assessment of both homogenization conditions and tip modification that enabled a highly reliable application of inocula. This opens the way to the use of vegetative mycelia as a source of inoculum in lieu of spores (19), the production of which might be a time-consuming procedure for basidiomycetes species, as opposed to ascomycetes and mitosporic fungi (34).

The smooth polystyrene surfaces of the pegs did not enable *P. ostreatus* biofilm formation, a finding in agreement with a previous study showing the inability of the fungus to adhere to this support under shaken conditions (21). The inadequacy of polystyrene for this purpose was also confirmed in other media, characterized by higher carbon/nitrogen ratios than in LB medium, and supplying readily available carbohydrates, such as either glucose or sucrose (21). Thus, the previous finding that the unfavorable nature of the contact surface for fungal biofilm settlement might be counteracted by the use of proper carbon sources in the growth medium (18) did not apply to *P. ostreatus*. Consequently, in the present study, HA coating of the pegs was definitely needed to allow biomass attachment, likely due to the higher wettability of HA and to the increase in surface roughness providing anchorage for the mycelium. With this adjustment, statistically equivalent *P. ostreatus* biofilms were obtained, thus meeting the stringent requirement for a reliable CBD-based susceptibility testing of toxicants. As opposed to the electroneutral polystyrene, HA, a hydrated calcium phosphate with the formula $Ca_{10}(PO_4)_6(OH)_2$, exhibits both positively and negatively charged ions. These charges might interact, at least in the initial phases of attachment, with functional groups on *P. ostreatus* cell walls via a mixed-mode ion exchange, as observed for HA chromatography (35). In a comparative study, HA best supported the biofilm growth of both *Candida glabrata* and *Candida albicans* (36). In addition, the inability of polystyrene pegs to gain satisfactory biofilm amounts was observed with the fungus *Candida tropicalis*, and coating with L-lysine was needed for this purpose (37).

In the present study, SEM analyses showed that the structural criteria, suggested by Harding et al. (2), were fully satisfied by *P. ostreatus* biofilms, although a 1-week incubation was required to attain a generalized ECM production abundantly lining constituent hyphae. Moreover, TEM observations showed the presence of secretory vesicles in close proximity to areas of the outer surfaces of hyphae where ECM accumulation had occurred. Chemical analyses of biofilms confirmed the time-dependent increase in extractable ECM (Fig. 2), observed by SEM, and showed that its composition mainly encompassed carbohydrates and, to a lesser extent, proteins, whereas neither lipids nor chitin were detected in agreement with Gutiérrez et al. (38).

CLSM was used in addition to SEM to investigate the biofilm structure since the dehydration steps required for specimens preparation in the latter technique have been suggested to severely distort biofilm architecture and to shrink any aqueous phase (39). Four-day-old *P. ostreatus* biofilms showed a highly heterogeneous structure displaying significant channeling and porosity. The presence of interstitial voids and channels in fungal biofilms was reported by other investigators and was suggested to represent an optimal structural arrangement to foster the influx of nutrients and the disposal of waste products (39, 40). A time-dependent change in the biomass distribution and hyphal organization of *P. ostreatus* biofilms was observed, with a notable increase in both the

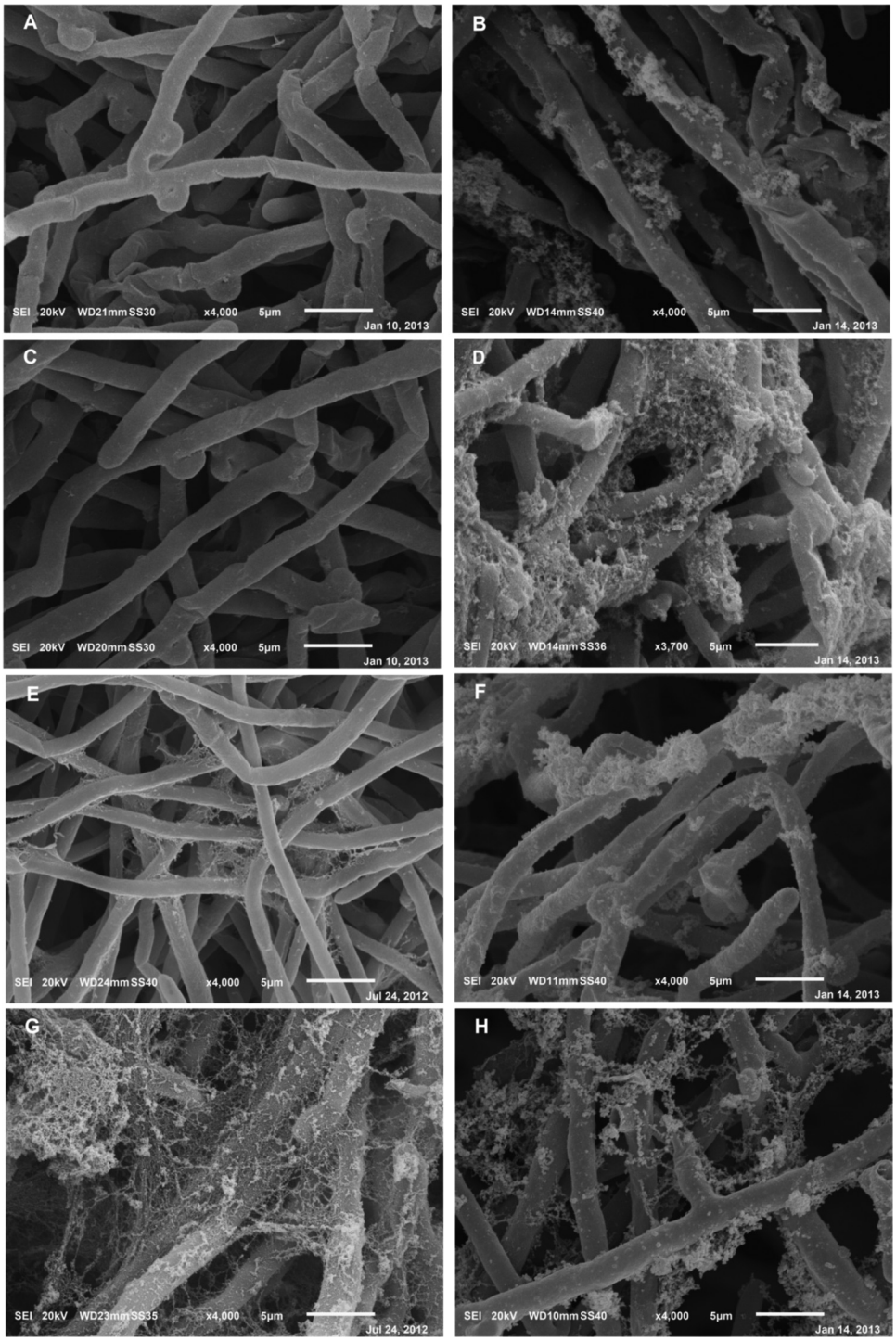

FIG 5 (A to F) SEM micrographs of unperturbed 4- and 7-day-old *P. ostreatus* free-floating (A and C, respectively) and biofilm (E and G, respectively) cultures compared to their respective counterparts (B and D, respectively, and F and H, respectively) exposed to cadmium concentrations equal to their IC_{90}s (see Table 1) at 30°C for 48 h in the LB medium under orbital shaking (150 rpm).

density and compactness of the mycelial network and the novel occurrence of large aggregates of ECM made only of α-glucan moiety enveloping hyphal components. A further time-dependent change was a preferential accumulation of components with α-glucan moiety in the innermost sections of 7-day-old biofilms, while both chitin or β-glucans appeared to predominate in the outermost ones (Fig. 4E, *xz* and *yz* side views). In another study, Di Bonaventura et al. (40) also showed that the network of active fungal cells in biofilms of the basidiomycete *Trichosporon asahii* was completely encased within an ECM composed of α-glucans.

However, in the present study, the red fluorescence emission was also found to be associated with hyphae. In this respect, although β-glucans and chitin are known to be major components of the *P. ostreatus* cell wall, a low-molecular-weight glucan with α-(1g4) and α-(1g6) glycosidic linkages was recently extracted from its vegetative mycelium by hot water extraction (41).

Conversely, and regardless of the incubation time, both chemical analyses (Fig. 2) and SEM observations (Fig. 5A and C) showed that free-floating biomasses were characterized by very low amounts of ECM. In particular, the mycelial agglomerates of free-floating cultures, evident as either spherical or pseudospherical pellets, were not characterized by the presence of abundant ECM encasing hyphae and acting as a cementing tool of these structures. Thus, in this respect, the main structural requisite of biofilms was not satisfied by *P. ostreatus* pellets. A similar comparison was performed by Villena and Gutiérrez-Correa (42), who found significant morphological dissimilarities between *Aspergillus niger* biofilms and pellets that were, in turn, correlated with differences in volumetric and specific productivities of several glycosyl hydrolases.

As an additional criterion of differentiation between *P. ostreatus* free-floating and biofilm cultures, the respective tolerances to toxicants were comparatively determined. To this aim, cadmium was chosen due to both its environmental ubiquity and high toxicity toward white-rot fungi (43, 44). A previous evaluation of metal toxicity to a given organism, relevant to bioremediation, is crucial to the successful design of biomining and mycoaugmentation applications, the latter being often applied to scenarios wherein organic contaminants are frequently intermingled with metals. For instance, Cd is often present in soil as a component of mixed contamination with polycyclic aromatic hydrocarbons (13) and can thus affect soil mycoremediation applications relying on *P. ostreatus* (12).

In general, toxic metal species kill biofilm populations in a time- and concentration-dependent manner. With regard to the first variable, the extents of increased tolerance of biofilm cultures with respect to free-floating counterparts tended to decrease as the exposure time was increased from 5 to 24 h (10, 29). Thus, to perform a reliable assessment of differential susceptibility of the two culture systems to Cd, the duration of the exposure to the metal was set at 48 h in the present study. In general, *P. ostreatus* free-floating cultures appeared to be rather susceptible to Cd inhibition in agreement with the study by Baldrian and Gabriel (45), who reported an IC_{50} as low as 0.18 mM for this species. In the present study, free-floating cultures in mid-exponential phase were much more tolerant to Cd than those in the stationary phase, as inferred by the respective MIC and MFC values. It might be speculated that the synthesis of nonenzymatic and enzymatic antioxidants and chelator compounds was more intense in the former than in the latter phase. However, an assessment of this hypothesis was outside the scope of the present study. Both MIC and MFC values clearly indicated that *P. ostreatus* biofilms exhibited a significantly higher tolerance to the metal than coeval free-floating cultures. SEM analyses of the latter, exposed to Cd^{2+} at MIC_{90}, showed the occurrence of stress phenomena, such as significant turgor losses (Fig. 5B), which were not evident in the former. These findings are in agreement with other studies reporting that the sessile growth mode might lead to a lower susceptibility to metal ions than the free-living mode (37, 46). Thus, in addition to fulfilling the structural criteria suggested by Harding et al. (2), *P. ostreatus* biofilms exhibited a commonly observed hallmark among microbial biofilms, namely, an increased resistance to toxicants compared to the respective free-floating state (2, 11). The combined action of chemical, physical, and physiological phenomena is the determinant for the increased tolerance to toxicants of biofilm systems compared to free-living counterparts (37). In some cases, it has been suggested that the reduced susceptibility of biofilms to toxic metals is associated with the natural process of phenotypic diversification that occurs within the biofilm population. In basidiomycetes, as opposed to *Candida* biofilms, the occurrence of specialized cells called persisters, mediating population multidrug and multimetal tolerance, has not yet been demonstrated (47). However, there is general agreement on the presence of metabolic gradients within solid surface-attached biofilms, which are mainly due to a restricted diffusion of nutrients, oxygen, and metabolites throughout the biofilm thickness. This results in uneven pH, redox poise conditions, and the occurrence of slow-growing subpopulations closest to the adhesion support facing anoxic conditions and exhibiting an intrinsic tolerance to killing by toxicants compared to the aerobic fast growers in the outer-biofilm layers (48, 49). In this respect, the occurrence of metabolic stratification in *P. ostreatus* biofilms might explain why 7-day-old biofilms, characterized by large thickness values, were more tolerant than the 4-day-old biofilms.

An additional determinant for the increased tolerance of fungal biofilms is the restricted diffusion and/or penetration of antimicrobials containing charged moieties, such as metal ions, into the biofilm matrix (37). The self-produced and hydrated ECM, encasing fungal biofilms and bearing a polyionic charge due to the presence of several substituents (e.g., carboxylate, phosphate, sulfhydryl, and amino groups) might act on sorption of metals via a variety of mechanisms involving ion exchange and formation of coordination complexes. As a matter of fact, *P. ostreatus* was able to perform Cd accumulation mainly via both biosorption and intracellular uptake (50).

In conclusion, we showed here for the first time the possibility of obtaining uniformly distributed *P. ostreatus* biofilms on the CBD, thus opening the way to a high-throughput evaluation of exposure conditions. The biofilms of this species clearly differed from their respective free-floating biomasses in terms of chemical composition, ultrastructure, and tolerance to cadmium. Although some studies seem to suggest that, regardless of the adhesion onto a surface, some mycelial aggregates might be regarded as biofilms, *P. ostreatus* pellets did not appear to satisfy structural biofilm requirements. It is becoming increasingly clear that biofilms of white-rot basidiomycetes have relevant applicative implications (5–10, 51); however, the information on these systems is still limited. We sought here to partially fill this gap and to provide a valuable basis for future studies.

ACKNOWLEDGMENT

This study was supported by the Ministero dell'Istruzione dell'Università e della Ricerca (MIUR) within project 2008P7K379.

REFERENCES

1. **O'Toole GA, Kaplan HB, Kolter R.** 2000. Biofilm formation as microbial development. Annu. Rev. Microbiol. **54:**49–79.
2. **Harding MW, Marques LL, Howard RJ, Olson ME.** 2009. Can filamentous fungi form biofilms? Trends Microbiol. **17:**475–480.
3. **Mowat E, Williams C, Jones B, Mcchlery S, Ramage G.** 2008. The

characteristics of *Aspergillus fumigatus* mycetoma development: is this a biofilm? Med. Mycol. **47**(Suppl 1):S120–S126.
4. **Beauvais A, Schmidt C, Guadagnini S, Roux P, Perret E, Henry C, Paris S, Mallet A, Prévost MC, Latgé JP.** 2007. An extracellular matrix glues together the aerial-grown hyphae of *Aspergillus fumigatus*. Cell Microbiol. **9:**1588–1600.
5. **Wu J, Xiao Y-Z, Yu H-Q.** 2005. Degradation of lignin in pulp mill wastewaters by white-rot fungi on biofilm. Bioresour. Technol. **96:**1357–1363.
6. **Jayasinghearachchi HS, Seneviratne G.** 2006. Fungal solubilization of rock phosphate is enhanced by forming fungal-rhizobial biofilms. Soil Biol. Biochem. **38:**405–408.
7. **Jayasinghearachchi HS, Seneviratne G.** 2006. A mushroom-fungus helps improve endophytic colonization of tomato by *Pseudomonas fluorescens* through biofilm formation. Res. J. Microbiol. **1:**83–89.
8. **Ragunathan R, Swaminathan KS.** 2004. Biological treatment of a pulp and paper industry effluent by *Pleurotus* spp. World J. Microbiol. Biotechnol. **20:**389–393.
9. **Jayasinghearachchi HS, Seneviratne G.** 2004. Can mushrooms fix atmospheric nitrogen? J. Biosci. **29:**293–296.
10. **Harrison JJ, Turner RJ, Ceri H.** 2005. Persister cells, the biofilm matrix and tolerance to metal cations in biofilm and planktonic *Pseudomonas aeruginosa*. Environ. Microbiol. **7:**981–994.
11. **Booth SC, Workentine ML, Wen J, Shaykhutdinov R, Vogel HJ, Ceri H, Turner RJ, Weljie AM.** 2011. Differences in metabolism between the biofilm and planktonic response to metal stress. J. Proteome Res. **10:**3190–3199.
12. **Baldrian P, in der Wiesche C, Gabriel J, Nerud F, Zadrazil F.** 2000. Influence of cadmium and mercury on activity of ligninolytic enzymes and degradation of polycyclic aromatic hydrocarbons by *Pleurotus ostreatus* in soil. Appl. Environ. Microbiol. **66:**2471–2478.
13. **Koeleman M, Ietswaart H, van der Laak WJ.** 1999. Dispersion of PAH and heavy metals along motorways in The Netherlands: an overview. Sci. Total Environ. **235:**347–349.
14. **Beyersmann D.** 1994. Interactions in metal carcinogenicity. Toxicol. Lett. **72:**333–338.
15. **Zeng X, Tang J, Yin H, Liu X, Jiang P, Liu H.** 2010. Isolation, identification and cadmium adsorption of a high cadmium-resistant *Paecilomyces lilacinus*. Afr. J. Biotechnol. **9:**6525–6533.
16. **Ceri H, Olson ME, Stremick C, Read RR, Morck D, Buret A.** 1999. The Calgary Biofilm Device: new technology for rapid determination of antibiotic susceptibilities of bacterial biofilms. J. Clin. Microbiol. **37:**1771–1776.
17. **Harrison JJ, Ceri H, Stremick CA, Turner RJ.** 2004. Biofilm susceptibility to metal toxicity. Environ. Microbiol. **6:**1220–1227.
18. **Parahitiyawa NB, Samaranayake YH, Samaranayake LP, Ye J, Tsang PWK, Cheung BPK, Yau JYY, Yeung SKW.** 2006. Interspecies variation in *Candida* biofilm formation studied using the Calgary biofilm device. APMIS **114:**298–306.
19. **Pierce CG, Uppuluri P, Tristan AR, Wormley FL, Mowat E, Ramage G, Lopez-Ribot JL.** 2008. A simple and reproducible 96-well plate-based method for the formation of fungal biofilms and its application to antifungal susceptibility testing. Nat. Protoc. **3:**1494–1500.
20. **Tremaroli V, Fedi S, Turner RJ, Ceri H, Zannoni D.** 2008. *Pseudomonas pseudoalcaligenes* KF707 upon biofilm formation on a polystyrene surface acquire a strong antibiotic resistance with minor changes in their tolerance to metal cations and metalloid oxyanions. Arch. Microbiol. **190:**29–39.
21. **Pesciaroli L, Petruccioli M, Federici F, D'Annibale A.** 2013. *Pleurotus ostreatus* biofilm-forming ability and ultrastructure are significantly influenced by growth medium and support type. J. Appl. Microbiol. **114:**1750–1762.
22. **Hawser SP, Douglas LJ.** 1994. Biofilm formation by *Candida* species on the surface of catheter materials in vitro. Infect. Immun. **62:**915–921.
23. **Roe JH.** 1955. The determination of sugar in blood and spinal fluid with anthrone reagent. J. Biol. Chem. **212:**335–343.
24. **Chen GC, Johnson BR.** 1983. Improved colorimetric determination of cell wall chitin in wood decay fungi. Appl. Environ. Microbiol. **46:**13–16.
25. **Izard J, Limberger RJ.** 2003. Rapid screening method for quantitation of bacterial cell lipids from whole cells. J. Microbiol. Methods **55:**411–418.
26. **Phillips MW, Gordon GLR.** 1989. Growth characteristics on cellobiose of three different anaerobic fungi isolated from the ovine rumen. Appl. Environ. Microbiol. **55:**1695–1702.
27. **Bradford MM.** 1976. A rapid and sensitive method for quantitation of microgram quantities of protein utilizing the principle of protein-dye binding. Anal. Biochem. **72:**248–254.
28. **Liu H, Fang HHP.** 2002. Extraction of extracellular polymeric substances (EPS) of sludges. J. Biotechnol. **95:**249–256.
29. **Harrison JJ, Turner RJ, Ceri H.** 2005. High-throughput metal susceptibility testing of microbial biofilms. BMC Microbiol. **5:**53. doi:10.1186/1471-2180-5-53.
30. **Karnovsky MS.** 1965. A formaldehyde-glutaraldehyde fixative of high osmolality for use in electron microscopy. J. Cell Biol. **27:**137–138.
31. **Kellenberger E, Ryter A.** 1958. Cell wall and cytoplasmic membrane of *Escherichia coli*. J. Biophys. Biochem. Cytol. **4:**323–326.
32. **Harrison JJ, Ceri H, Yerly J, Stremick CA, Hu Y, Martinuzzi R, Turner RJ.** 2006. The use of microscopy and three-dimensional visualization to evaluate the structure of microbial biofilms cultivated in the Calgary Biofilm Device. Biol. Proc. Online **8:**194–215.
33. **Albani JR, Plancke YD.** 1999. Interaction between calcofluor white and carbohydrates of alpha 1-acid glycoprotein. Carbohydr. Res. **318:**194–200.
34. **Choi YW, Hyde KD, Ho WH.** 1999. Single spore isolation of fungi. Fungal Divers. **3:**29–38.
35. **Dennison C.** 2003. Hydroxyapatite chromatography, p 128–141. *In* Dennison C (ed), A guide to protein isolation. Kluwer Academic Publishers, Dordrecht, Netherlands.
36. **Pereira-Cenci T, Deng DM, Kraneveld EA, Manders EM, Del Bel Cury AA, Ten Cate JM, Crielaard W.** 2008. The effect of *Streptococcus* mutants and *Candida glabrata* on *Candida albicans* biofilms formed on different surfaces. Arch. Oral Biol. **53:**755–764.
37. **Harrison JJ, Rabiei M, Turner RJ, Badry EA, Sproule KM, Ceri H.** 2006. Metal resistance in *Candida* biofilms. FEMS Microbiol. Ecol. **55:**479–491.
38. **Gutiérrez A, Prieto A, Martínez AT.** 1996. Structural characterization of extracellular polysaccharides produced by fungi from the genus *Pleurotus*. Carbohydr. Res. **281:**143–154.
39. **Chandra J, Kuhn DM, Mukherjee PK, Hoyer LL, McCormick T, Ghannoum MA.** 2001. Biofilm formation by the fungal pathogen *Candida albicans*: development, architecture, and drug resistance. J. Bacteriol. **183:**5385–5394.
40. **Di Bonaventura G, Pompilio A, Picciani C, Iezzi M, D'Antonio D, Piccolomini R.** 2006. Biofilm formation by the emerging fungal pathogen *Trichosporon asahii*: development, architecture, and antifungal resistance. Antimicrob. Agents Chemother. **50:**3269–3276.
41. **Lavi I, Friesem D, Geresh S, Hadar Y, Schwartz B.** 2006. An aqueous polysaccharide extract from the edible mushroom *Pleurotus ostreatus* induces anti-proliferative and proapoptotic effects on HT-29 colon cancer cells. Cancer Lett. **244:**61–70.
42. **Villena GK, Gutiérrez-Correa M.** 2007. Morphological patterns of *Aspergillus niger* biofilms and pellets related to lignocellulolytic enzyme productivities. Lett. Appl. Microbiol. **45:**231–237.
43. **Baldrian P.** 2003. Interactions of heavy metals with white-rot fungi. Enzyme Microb. Technol. **32:**78–91.
44. **Ezzouhri L, Castro E, Moya M, Espinola F, Lairini K.** 2009. Heavy metal tolerance of filamentous fungi isolated from polluted sites in Tangier, Morocco. Afr. J. Microbiol. Res. **3:**35–48.
45. **Baldrian P, Gabriel J.** 1997. Effect of heavy metals on the growth of selected wood-rotting basidiomycetes. Folia Microbiol. (Praha) **42:**521–523.
46. **Harrison JJ, Ceri H, Turner RJ.** 2007. Multimetal resistance and tolerance in microbial biofilms. Nat. Rev. Microbiol. **5:**928–938.
47. **Lafleur MD, Kumamoto CA, Lewis K.** 2006. *Candida albicans* biofilms produce antifungal tolerant persister cells. Antimicrob. Agents Chemother. **50:**3839–3846.
48. **Walters MC, III, Roe F, Bugnicourt A, Franklin MJ, Stewart PS.** 2003. Contributions of antibiotic penetration, oxygen limitation, and low metabolic activity to tolerance of *Pseudomonas aeruginosa* biofilms to ciprofloxacin and tobramycin. Antimicrob. Agents Chemother. **47:**317–323.
49. **Borriello G, Werner E, Roe F, Kim AN, Ehrlich GD, Stewart PS.** 2004. Oxygen limitation contributes to antibiotic tolerance of *Pseudomonas aeruginosa* in biofilms. Antimicrob. Agents Chemother. **48:**2659–2664.
50. **Favero N, Costa P, Massimino ML.** 1991. *In vitro* uptake of cadmium by basidiomycete *Pleurotus ostreatus*. Biotechnol. Lett. **13:**701–704.
51. **Ntwampe SKO, Sheldon MS.** 2006. Quantifying growth kinetics of *Phanerochaete chrysosporium* immobilised on a vertically orientated polysulphone capillary membrane: biofilm development and substrate consumption. Biochem. Engl. J. **30:**147–151.